ISSN 1349-1113
JAXA-RR-06-009E

JAXA Research and Development Report

Design of Sub-Scale Rocket-Ramjet Combined Cycle Engine Model

Takeshi KANDA , Sadatake TOMIOKA , Shuichi UEDA and Kouichiro TANI

February 2007

Japan Aerospace Exploration Agency

JAXA-RR-06-009E

JAXA Research and Development Report
宇宙航空研究開発機構研究開発報告

Design of Sub-Scale Rocket-Ramjet Combined Cycle Engine Model

ロケット-ラムジェット複合サイクルエンジン・サブスケールモデルの設計

Takeshi KANDA , Sadatake TOMIOKA , Shuichi UEDA and Kouichiro TANI

苅田　丈士、富岡　定毅、植田　修一、谷　香一郎

Combined Propulsion Research Group, Institute of Aerospace Technology
総合技術研究本部　複合推進研究グループ

February 2007
2007年2月

Japan Aerospace Exploration Agency
宇宙航空研究開発機構

Design of Sub-Scale Rocket-Ramjet Combined Cycle Engine Model

Takeshi Kanda,* Sadatake Tomioka,* Shuichi Ueda,* and Kouichiro Tani*

Abstract

A sub-scale rocket-ramjet combined cycle engine model was designed and will be tested at the Ramjet Engine Test Facility under sea-level static, Mach 4, 6 and 8 flight conditions. The engine operates in the ejector-jet, ramjet, scramjet and rocket modes and this model has two H_2-O_2 rockets in the duct. Fuel injectors for secondary combustion have been installed in the downstream straight duct section. Each component of the engine was examined experimentally and physical models were constructed. The engine model is 3 m long, 0.2 m high with a width of 0.22 m at the inlet entrance. The pressure level in the rocket chamber is 3 MPa, and net thrust is 4 kN under the sea-level static, design condition.

概　要

ラムジェットエンジン試験設備において地上静止大気条件、マッハ4飛行条件、マッハ6飛行条件およびマッハ8飛行条件で実験するサブスケールロケット-ラムジェット複合サイクルエンジン模型を設計した。ロケット-ラムジェット複合サイクルエンジンはエジェクタージェットモード、ラムジェットモード、スクラムジェットモードおよびロケットモードで作動する。エンジン模型は内部にふたつの水素／酸素ロケットを有している。下流平行部には、二次燃焼用の燃料噴射器がある。エンジンのそれぞれの構成要素は、実験的に検討され、必要な物理モデルを構築した。エンジン模型の長さは3 mであり、入口部で高さ0.2 m、幅0.22 mである。ロケット燃焼器圧力は3 MPaであり、このときの地上静止状態での設計正味推力は4 kNである。

Nomenclature

A	= cross section
F	= impulse function
f	= force
H	= height
L	= length
M	= Mach number
m	= mass flow rate
P	= pressure
x	= distance
ϕ	= equivalence ratio

Subscript

a	= air
c	= rocket combustion chamber
ch	= choking condition
div	= divergent duct
e	= outflow, exit
i	= inflow
f	= friction
p	= pseudo-shock
r	= reaction, rocket
t	= total
w	= wall
0	= stagnation
1	= primary flow, region upstream of pseudo-shock
2	= secondary flow

*Combined Propulsion Research Group, Institute of Aerospace Technology（総合技術研究本部　複合推進研究グループ）
Received 8 December, 2006（平成18年12月8日受付）

1. Introduction

The current space transportation system is based on the rocket engine. Its performance, that is, its specific impulse, has almost reached a theoretical limit. A new transportation system with a new engine is required to attain an increase of transportation ability, a decrease of transportation cost, and an increase of reliability.[1] An oxygen mass ratio of most of launch rockets is 70%. Use of a suitable air-breathing engine will reduce the ratio of the carrying oxidizer and increase a mass ratio of payload or a ratio of the vehicle structure. Since kinetic energy of a space vehicle is larger than potential energy in an orbit, acceleration with the air-breathing engine to supersonic or hypersonic speed is effective to reduce the oxidizer mass ratio. The ramjet engine is effective to accelerate in a hypersonic speed range, but cannot operate in a subsonic or transonic speed range. Combined-cycle engines including the rocket engine are effective to accelerate in the low speed range and in space. Thus the rocket-ramjet combined-cycle engine is effective in space transportation. This engine is known as the Rocket Based Combined Cycle (RBCC) engine and the most famous one is the strut jet.[2] The engine has been studied for the advanced space transportation system.[3-5]

The engine works in several operating modes. The engine can be applied to a booster engine of the traditional rocket, which increases specific impulse of a booster stage. The combined-cycle engine will also be used in a hypersonic observation vehicle or a hypersonic test vehicle. The vehicle cruises in a hypersonic speed, or flies-up to an altitude around 100 km by transforming kinetic energy to potential energy.

The Japan Aerospace Exploration Agency (JAXA) has studied the rocket-ramjet combined-cycle engine. The engine has rocket modules inside the engine duct, and operates in an ejector-jet mode, also known as, an air-breathing rocket mode, as well as ramjet, scramjet and rocket modes.[6] The engine can fly a space transportation vehicle from take-off to space, or accelerate it from take-off to a hypersonic speed. Figure 1 shows an image of the vehicle with the combined-cycle engine.

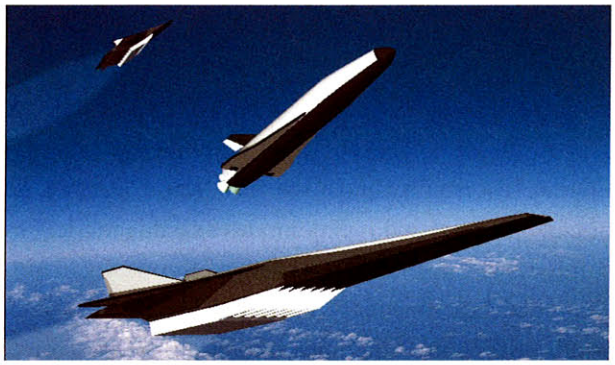

Fig. 1 An image of vehicles with the combined-cycle engine.

A rocket-ramjet combined-cycle engine model is designed and is now under construction to validate the component research results, to demonstrate each operating condition and to establish design technologies of the rocket-ramjet combined-cycle engine. The model will be tested under the sea-level static, Mach 4, Mach 6 and Mach 8 conditions in the Ramjet Engine Test Facility (RJTF) of JAXA. Table 1 lists the test conditions. About 0.25 m × 0.25 m × 3 m engine model can be installed in the test chamber with a 0.5 m × 0.5 m facility nozzle. The facility has a gas hydrogen supply system for combustion tests. During an experiment, temperature of 60 points, pressure of 300 points and thrust force can be measured simultaneously. RJTF is equipped with a high temperature gas supply system and an ejector system. High temperature gas is created by the storage air heater with hot pebbles (SAH) and /or the vitiated air heater which utilizes hydrogen and oxygen chemical reaction (VAH). RJTF can supply water at 20×10^{-3} $m^3 \cdot s^{-1}$ to cool the engine model. In the present paper, reference research results and design procedure of this engine model are described.

Table 1 Flow conditions of RJTF

Flight Mach No.	Mach No. at entrance	Air heater	Total temperature, K	Total pressure, MPa
4	3.4	SAH	800	0.8
6	5.4	SAH	1500	5.0
6	5.2	VAH	1500	4.5
8	6.7	SAH+VAH	2400	10.0

2. Rocket-Ramjet Combined-Cycle Engine

The operating conditions of the rocket-ramjet combined-cycle engine are explained in this chapter. Figure 2 shows a schematic of the operating conditions, and Figure 3 shows a picture of a display model.

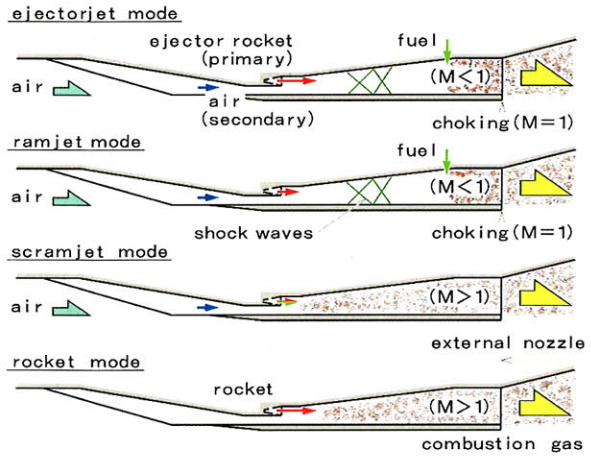

Fig. 2 Schematic of operating conditions of combined- cycle engine.

The engine operates in the ejector-jet mode from take-off to about Mach 3. Under the ejector-jet mode, air is breathed in by the ejector effect of the rocket. Rocket exhaust and breathed airflow are decelerated to subsonic speed through the pseudo-shock. Thrust is produced not only by the rocket engine itself, but also by the divergent section with the increased pressure of a mixture of air and rocket exhaust. Further subsonic combustion is attained by fuel injection from a second fuel injector.

From about Mach 3 to 7, the engine operates in the ramjet mode. In the ramjet mode, the rocket exhaust decreases, and pressure recovery of the air is attained in the divergent section through the pseudo-shock. There are two kinds of the ramjet modes. One is the downstream ramjet mode indicated in Fig. 2.[7] Another is the upstream-combustion ramjet mode, which is a ramjet mode of the dual-mode engine.[8,9] In the upstream-combustion ramjet mode, the inflow supersonic airflow decelerates to subsonic speed in the throat section downstream of the inlet. Fuel is injected to the subsonic air. Combustion gas accelerates to sonic speed and chokes at the exit of the straight duct section. Combustion position and pressure distribution are similar to those of the scramjet mode.

From about Mach 7 to 12, the engine operates in the scramjet mode. In the scramjet mode, the ejector rockets work as a pre-burner to supply hot, fuel-rich gas. When the vehicle cruises, the flow rate of rocket exhaust is suppressed and specific impulse is increased. When the vehicle accelerates, thrust of the rocket and thrust of the engine are increased with a large amount of rocket exhaust.[10] When the engine flies the aerospace plane to an orbit, the engine operates in the rocket mode above about Mach 12. When the engine is applied to a booster stage of the two stage aerospace plane, the engine operates in the rocket mode during pull-up flight prior to the staging.

Ejector rocket engines are mounted in the inlet ramp. A propellant feed system with umbilical ducts from the cryogenic propellant tanks is mounted in the ejector rocket section. This is the heaviest section of the engine and is difficult to have a variable geometry. In the display engine model of Fig. 3 and in the conceptual study, [6] this section and the following combustor section are fixed and the contraction of the inlet is also fixed during operation. The inlet has a ramp-compression system. The ramp is movable and closes the inlet in the entry flight from an orbit when applied to a single stage aerospace plane.[11]

In the display engine model of Fig. 3 and in the conceptual study, there is no second throat at the exit of the engine. Subsonic combustion in the absence of a second throat configuration with choking was attained

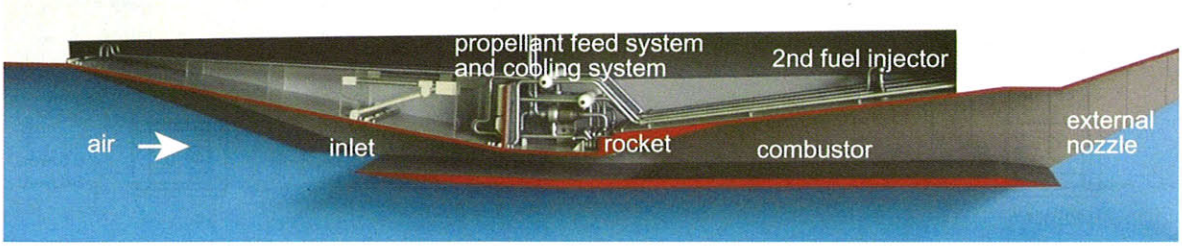

Fig. 3 Display model of a rocket-ramjet combined-cycle engine.

in the experiments of the ramjet mode operation.[7,12] With no second throat, the engine can be simplified and is lighter. However, high equivalence ratio is required to attain the choking condition at the engine exit with no throat.

3. Reference Results and Design of Model Engine

3.1. Design guide line

Figure 4 shows a schematic of the engine model under construction. Cross section of the engine is rectangular and the engine duct is constructed with plates for convenience of changing each part to another. The engine may not have a variable configuration, then an actual engine will not have to be constructed with flat plates except the inlet.

The contraction ratio of the inlet is a major parameter of the engine, and is specified to 4.9. This value is high from a viewpoint of an airflow rate in the ejector-jet mode, since the throat area becomes rather small. However, with smaller amount of air with this ratio, the ejector effect will be attained with small trouble. Such a high ratio of the contraction is preferable to production of thrust in high Mach numbers. There is base area due to the installment of the rocket nozzles, so the area ratio of the engine entrance to the upstream combustor section becomes smaller than the inlet contraction ratio. Larger ratio to the upstream combustor section is preferable to produce larger thrust in the divergent section. However, due to the size of the rocket, the current model has a limit of the ratio which is rather small.

Rocket engines are mounted inside the inlet-ramp housing. Two rockets are mounted in the engine. A large number of small rocket engines with a square nozzle are preferable to increase the divergent cross section downstream of the rockets. However, small rocket engine is difficult to be cooled, and the square nozzle is difficult to be made and will be expensive. In the present model, the number is reduced to two with a round nozzle.

Propellants are gas hydrogen and gas oxygen, which can be supplied in RJTF. Liquid oxygen cannot be supplied now. Coolant of the engine model is water. In the model, fuel injectors will be located in the divergent section on the sidewalls and cowl, as well as on the top wall in the downstream combustor. The fuel injection position will be a parameter in tests.[13]

The engine model under construction has a second throat to attain the choking condition around the stoichiometric fuel flow rate. Excessive fuel condition is avoided for safety. In the tests of the upstream-combustion ramjet mode, scramjet mode and the rocket mode, the second throat is not adopted. The model engine has a fixed-geometry inlet ramp, since the model is not designed for flight. The inlet will be designed in details and constructed in next financial year.

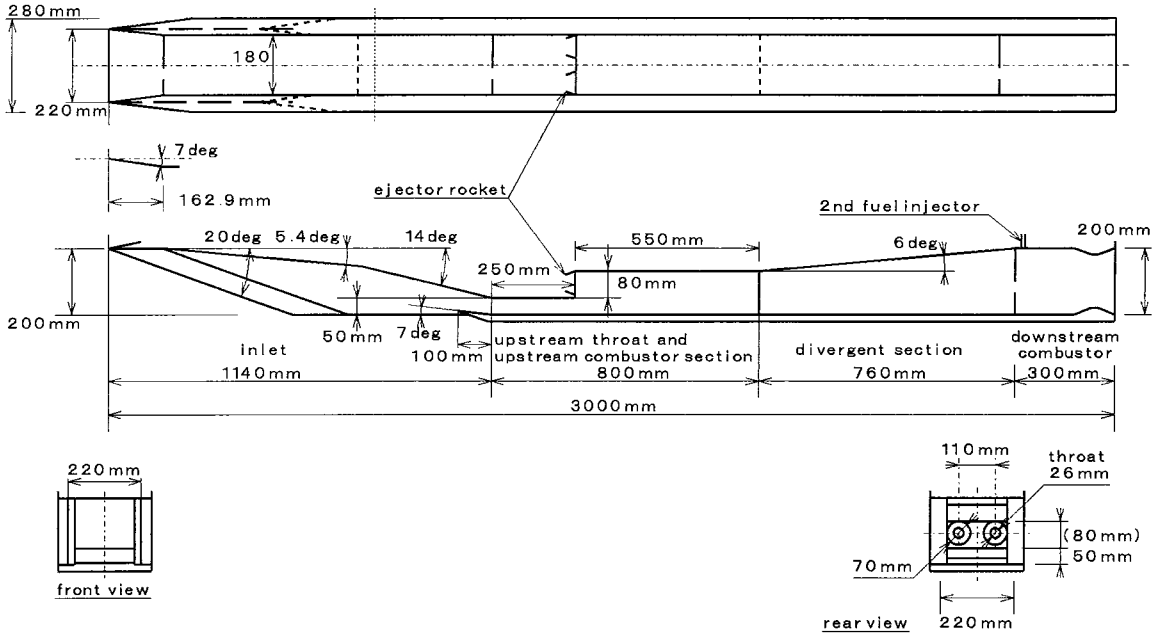

Fig. 4 Schematic of rocket-ramjet combined cycle engine model

3.2 Inlet section

The compression of the incoming air is achieved by the sidewall originated shock waves and the ramp shock wave. Here, the compression by the sidewall shock is referred as sidewall-compression, while that by the ramp shock is called ramp-compression. The reduction of the ratio of the sidewall-compression to the ramp-compression has an effect to increase the air capture ratio.[14] It also results to decrease the ramp angle. Larger ramp angle easily induces separation on the top wall. Here, the two-stage-ramp inlet is adopted. The angles of the first ramp and the second ramp from the horizontal line are 5.4 deg. and 14 deg, respectively. The sidewall has just enough thickness to contain ducts and tubes for cooling and measuring.

The cowl lip is turned up toward the top wall in 7 deg. Decreasing relative angle of the cowl inner surface to the inlet ramp suppresses pressure ratios by the shock wave from the cowl lip and by the reflected shock on the ramp. This makes the inlet to start in lower Mach numbers.[15]

Airflow through shock waves in the inlet increases its dynamic pressure. Heat flux to the cowl leading edge is largest in the airflow condition. Figure 5 shows a temperature distribution of the cowl leading edge at 30 s from staring of heating under the RJTF Mach 8 test condition.[16] The cowl was made of copper and cooled by water.

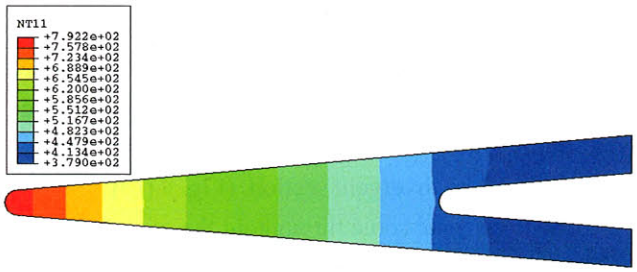

Fig. 5 Temperature distribution of the water-cooled Cu cowl leading edge at 30 s.

3.3. Rocket section

Figure 6 shows a schematic of the rocket chamber for validation tests. The rocket chamber and the rocket nozzle are designed for the operating condition under the ejector-jet mode. Maximum chamber pressure is set to be 5 MPa from propellant supply capacity of the RJTF and durability of the rocket. Mixture ratio of the rocket, $(O/F)_r$, at this mode is 7 to reduce the excess fuel in the plume and leave combustion in the downstream straight section by the secondary fuel injection. Thrust of 4 kN for each rocket chamber is sufficient for parametric operation in the tests, so the throat diameter is specified to be 26 mm. The exit diameter of the rocket nozzle is 70 mm, and the height of the rocket base is 80 mm. For the ejector-jet mode operation, a chamber pressure of 3 MPa and a thrust of 2 kN per a rocket are specified as nominal design conditions. Thus, the chamber pressure and the thrust have room to be raised. The diameter of the combustion chamber of the rocket is limited to be 50 mm due to the installation restriction. The upstream curvature radius at the throat was 32 mm to suppress excessive heat flux around the throat.[17] The downstream radius is 13 mm, relatively small due to the restriction of the total length of the rocket.

An igniter is located at the center of the rocket,[18] and 8 injectors are located around the igniter. The choking condition is applied in hydrogen and oxygen injectors to control the flow rates of propellants in a wide range of $(O/F)_r$. There is a diffuser section downstream of the choking point to recover pressure. Design Mach numbers of the propellants are 0.4.[19]

This rocket chamber should operate in a wide range of a mixture ratio to fulfill various mode operations. When the mixture ratio is reduced to 0.5 to realize a scramjet mode with high specific impulse, number of the oxygen injectors is reduced half. Throttling of the rocket thrust is also necessary to meet operation requirements including the reduced pressure condition.

Coolant is water to suppress production cost and to handle the chamber easily. The rocket chambers consist of inner wall of copper alloy, SMC(MOF-CZ), and outer wall of stainless steel by brazing, expensive process such as electro-forming being avoided. Fin is shaped in the cooling channel to enhance the cooling ability.[20]

Tests of the rocket chamber were conducted. Figure 7 shows plume in the ejector-jet mode operation. Figure 8 shows the summary of the chamber performance of C* at various operating modes.[21] In all cases, no oscillation associated with combustion was observed, but melting of the oxygen posts and part of the faceplate were experienced. New oxygen posts made of nickel and modified nickel faceplate were fabricated and melting was mitigated.

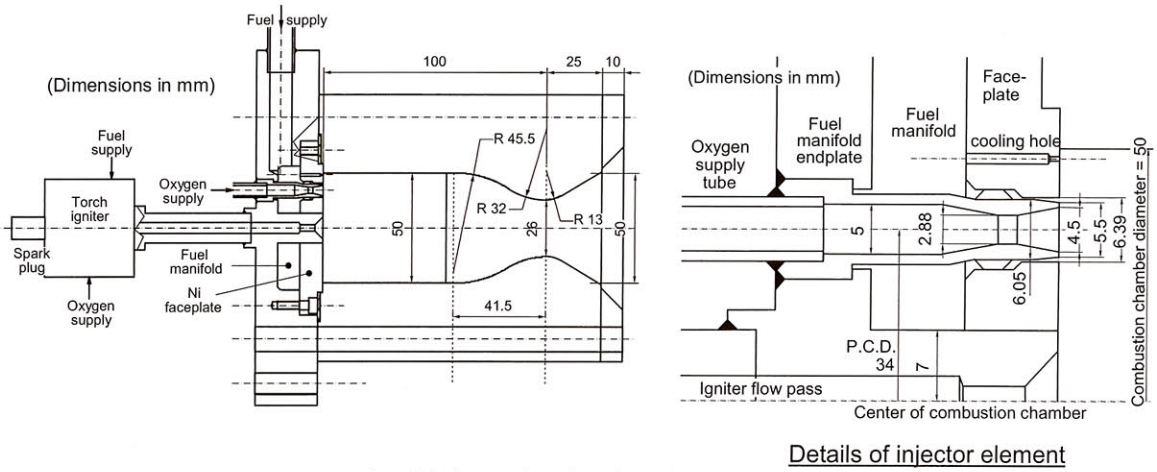

Fig. 6 Schematic of rocket chamber.

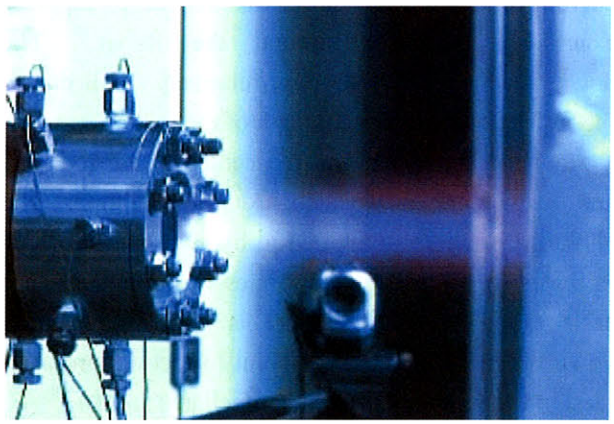

Fig. 7 Operation of rocket model

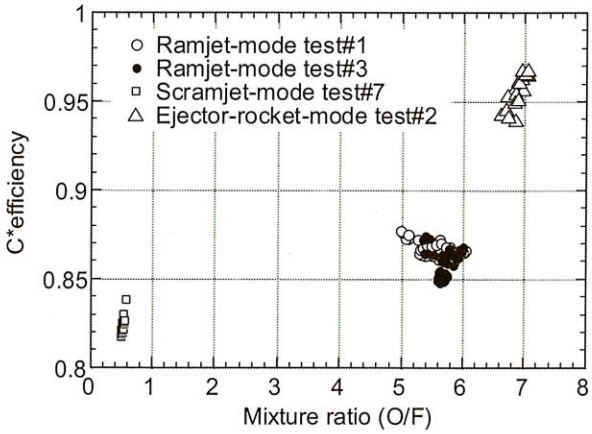

Fig. 8 C* efficiency summary.

3.4. Ejector section

In a low speed condition, air is breathed into the engine by the ejector effect of the rockets. From a viewpoint of the ejector effect, the section from the upstream throat to the upstream combustor is termed the ejector section here. The breathed air is used for secondary combustion and augmentation of the rocket thrust. The area ratio of the secondary flow to that of the primary flow, the pressure of the rocket chamber, and the nozzle area ratio of the rocket are primary parameters on the ejector effect. The area ratio has a relation to the contraction ratio of the inlet. The contraction ratio or the area ratio should be selected to attain sufficient airflow in lower Mach numbers, as well as sufficient thrust in higher Mach numbers.

The flow conditions of the breathed air can be categorized in three.

(1) Airflow chokes and then becomes supersonic or is supersonic at the exit of the throat section. The air flows in the supersonic speed in the divergent section, as well as the rocket exhaust. (Fig. 9 (a))

(2) Airflow is subsonic at the exit of the throat section, and chokes in the upstream combustor section due to aerodynamic interaction between the air and the rocket exhaust, i.e., the aerodynamic choking condition. The air and the rocket exhaust are supersonic in the divergent section. (Fig. 9 (b))

(3) Airflow is subsonic throughout the engine duct.

Though there are several models for the ejector effect, a simple model was newly-constructed. Its applicability was confirmed with comparison between the calculated values and the experimentally measured ones.[22] Exchange of momentum between the rocket exhaust and the breathed air in the aerodynamic choking condition was calculated with this simple model, which is noted as Model (c) in Figs. 10 (a) and (b), in the design process. Figs. 10 (a) and (b) shows the secondary mass flow rate normalized by the maximum secondary flow rate under the choking condition of the secondary flow at $M_1 = 2.4$.

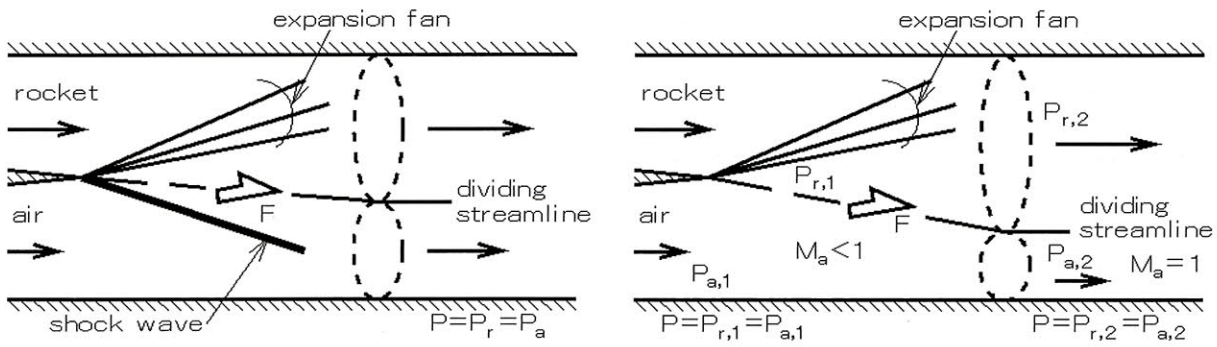

Fig. 9 Schematic of interaction between rocket exhaust (primary flow) and air (secondary flow). (a) Air is supersonic or chokes at entrance. (b) Aerodynamic choking condition. Subsonic air chokes aerodynamically.

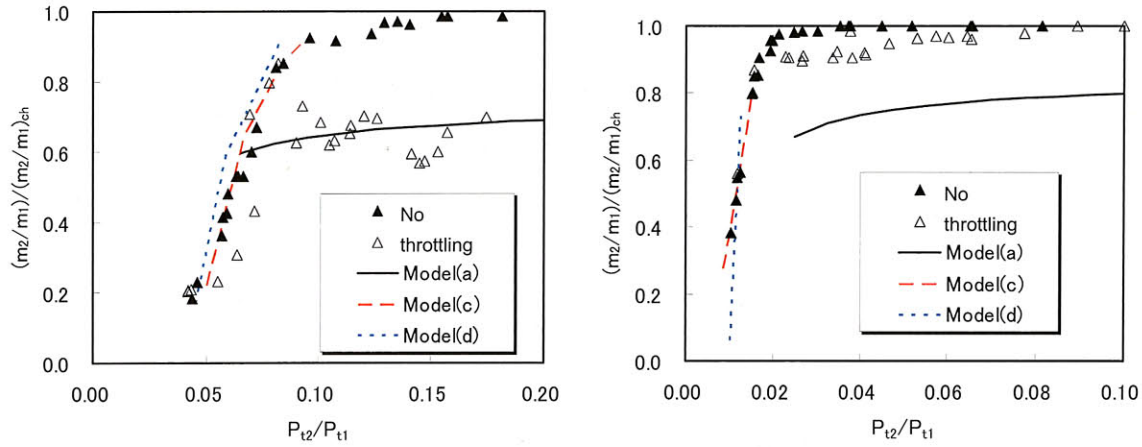

Fig. 10 Comparison of calculated results to experimental ones. M1 is Mach number of primary flow. A1 iscross section of primary flow, and A2 is that of secondary flow. ▲ expresses test condition with no exit throat, and Δ does the condition with exit throat for a downstream pressure increase. (a) M_1=2.4, A2/A1=0.57. (b) M_1=3.4, A2/A1=0.57.

The inlet contraction ratio is specified to be 4.9, as mentioned in Section 3.1. The choking condition of air due to the ejector effect will be attained even with P_c = 2.5 MPa, based on calculation with Model (c). In the calculation, rocket exhaust was presumed to flow parallel to the top wall of the engine duct with no thickness of split plate. Combustion efficiency of the rocket chamber was presumed to be unity.

The ejector effect of the model was confirmed with a small-sized, simplified-configuration model in a transonic wind tunnel under Mach 0.3 to Mach 1.1.[23] Figure 11 shows the model. At the mid of the model, nitrogen gas was provided through tubes to simulate rocket exhaust. Figure 12 shows sidewall pressure distributions in the Mach 0.8 test. With the exhaust of the rocket, at downstream of the rocket nozzle exit, wall pressure became lower than the choking pressure of air, which is denoted as a dotted horizontal line. Wall pressure increased to the total pressure of air and then the mixture choked at the exit.

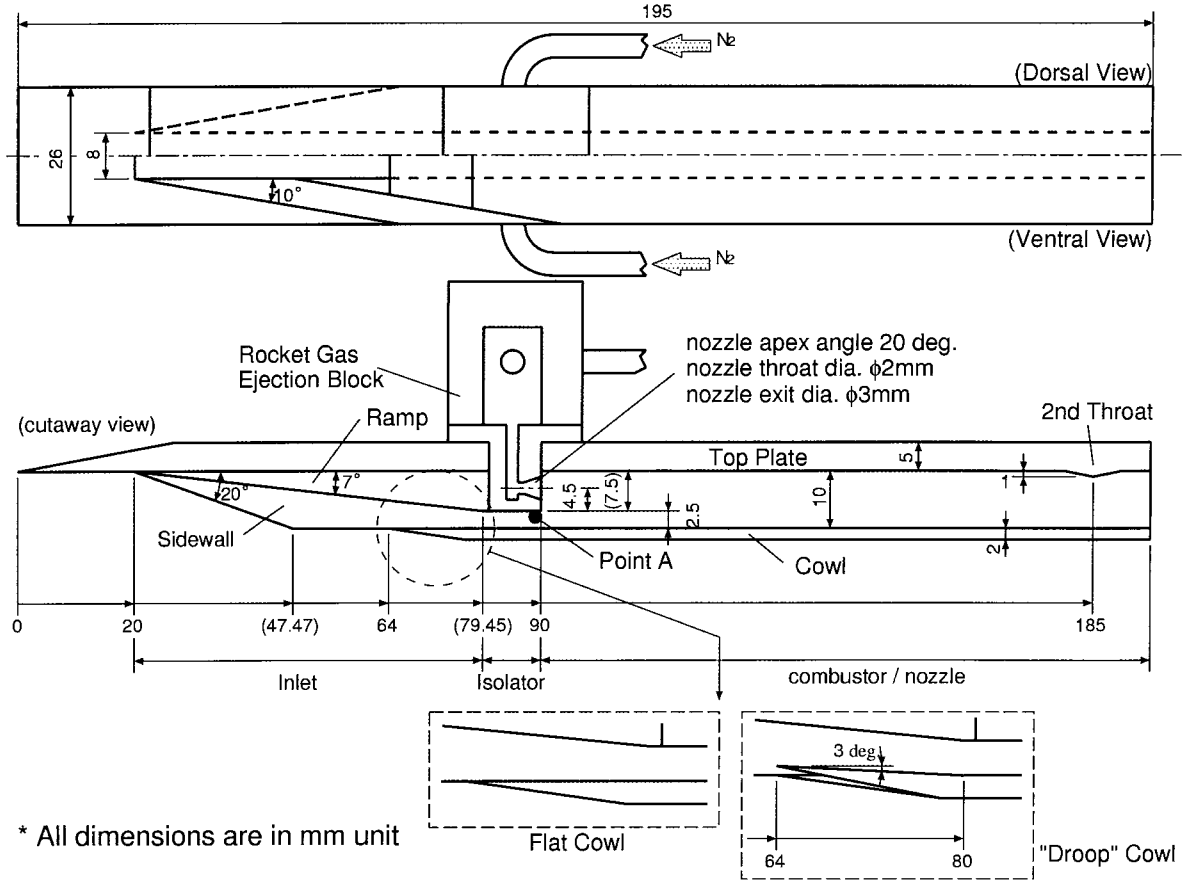

Fig. 11 Engine model for aerodynamic test. Rocket exhaust is simulated with N_2 gas.

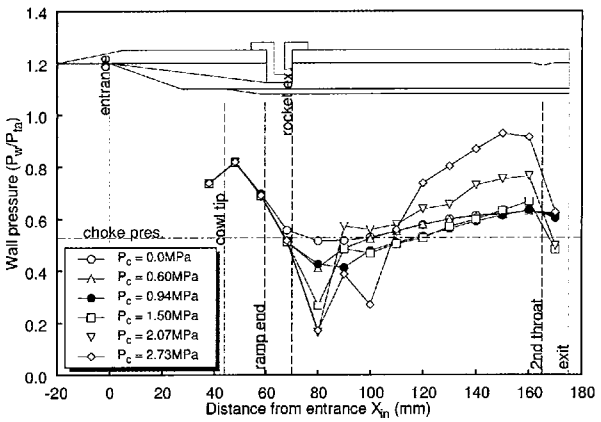

Fig. 12 Wall pressure distribution at Mach 0.8 condition.

3.5. Upstream combustor section

The upstream combustor consists of the rocket base and the downstream straight duct. As the rocket size and hence the rocket base size are fixed, the design parameter to be determined is the length of the straight duct. Two issues should be taken into account for the determination; the interaction length requirement for the ejector-jet mode operation, and the combustor length requirement for the scramjet mode operation in which the rocket engine is used as the fuel injector.

As for the former, an interaction region downstream of the rocket base position is required for sufficient interaction between the airflow and the rocket plume in order to realize the suction performance. Reflections of the expansion waves were necessary for sufficient acceleration of air, and the corresponding length was set for the straight duct.

Combustor tests in the scramjet mode conditions were conducted to determine the necessary straight duct length, as a certain ignition delay was expected in this operation mode. Figure 13 shows the schematic of the experimental model, and Figure 14 shows wall pressure distributions.[24] As results, it was found that specified length of the straight duct, L/H larger than 6.3, was required to attain sufficient combustion condition, i.e., onset of the pressure rise being at the rocket base region. The required length of the straight duct was reduced with auxiliary fuel injection from the cowl side. Figure 15 shows the wall pressure distributions with the auxiliary injection.[25] In this test,

L/H was 2.3, the shortest condition of the straight duct. Even with such a short duct, a good combustion condition was attained with the auxiliary fuel injection. Taking these into account, the ratio of the length of the upstream straight section to the height is specified to be about 4 in the engine model, shorter than 6.3. Such length of the duct would be required for sufficient reflection of expansion waves in the ejector section under the aerodynamic choking condition of the ejector jet mode. In the aerodynamic acceleration process of the breathed air, expansion waves are reflected on the wall of the rocket side and next on the dividing streamline between the rocket exhaust and the breathed air. The simplified model abbreviates this reflection of the waves in the aerodynamic choking condition shown in Fig. 9 (b).

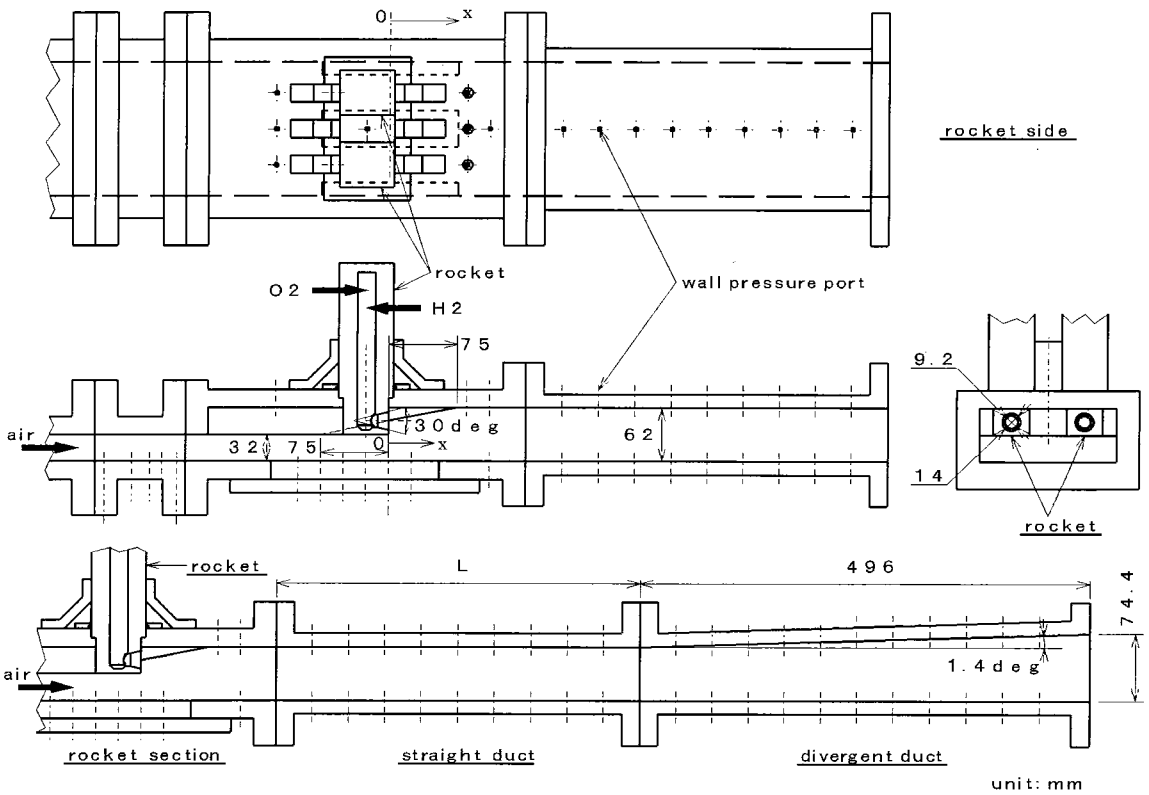

Fig. 13 Schematic of combined cycle engine combustor model.

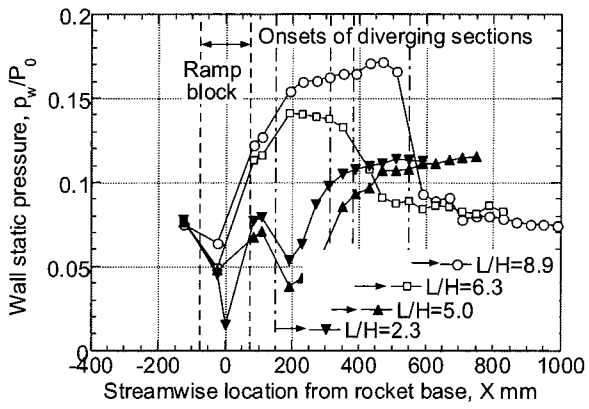

Fig. 14 Wall pressure distributions with different straight duct length.

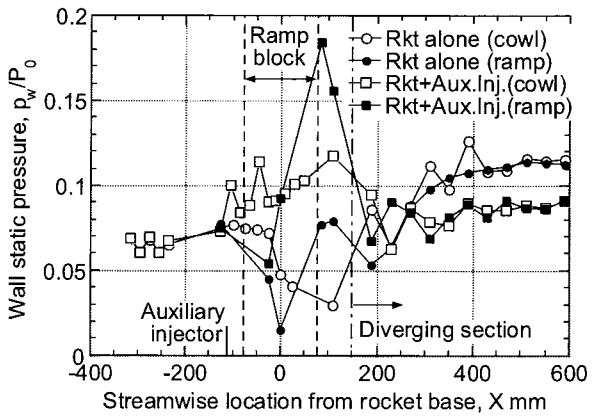

Fig. 15 Wall pressure distributions with auxiliary fuel injection from cowl side wall.

The auxiliary injector or the rocket engine operating as a fuel rich pre-burner can also be used in the upstream-combustion ramjet mode. This combustion condition is also expected as an operating mode of this engine. With additional fuel injection within the following diverging section, the subsonic, high-pressure region can be extended to further downstream into the diverging section to attain a higher thrust.[13]

3.6. Divergent section

In the ejector-jet and the ramjet modes, supersonic airflow and combustion gas decelerate and mix in this section through the pseudo-shock to subsonic speed. Increased pressure in the decelerating process produces thrust. The pressure increase and the length of the pseudo-shock were calculated with the momentum balance model.[26] In the model, there is no friction force in the pseudo-shock. The length is calculated with force balance in the duct with the pseudo-shock. Figure 16 shows a schematic of the pseudo-shock in a divergent duct. Balance of forces is described as follows;

$$F_e = F_i + f_r - f_{f1} \tag{1}$$

F_e, F_i, f_r, and f_{f1} are outflow impulse function, inflow impulse function, reaction force from wall in L_p, and friction force upstream of the pseudo-shock in L_{f1}. The lengths of L_p and L_{f1} are determined to satisfy Eq. (1) in the model.

Figure 17 shows a relation between calculated lengths and the measured ones. Values larger than unity express that the starting position of the pseudo-shock is in the straight section upstream of the divergent section.

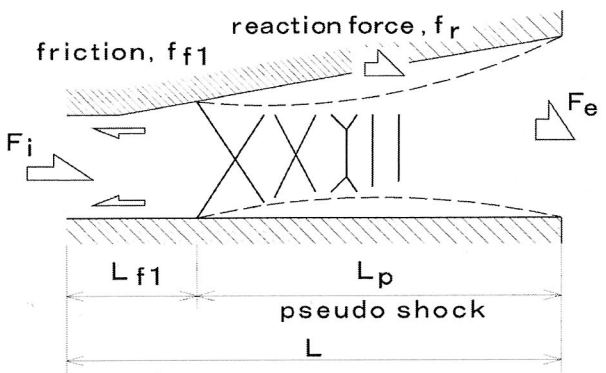

Fig. 16 Schematic of flow with pseudo-shock.

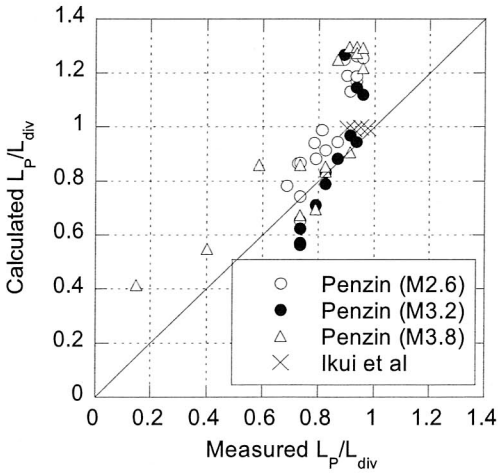

Fig. 17 Relation between calculated lengths of pseudo-shock and measured ones in divergent duct.

With the model, effect of the downstream throat contraction ratio, CR_e, and that of the rocket chamber pressure on the pseudo-shock length in the divergent duct section of the new engine model were predicted in the ejector-jet mode (Figs. 18 and 19). The calculated lengths dispersed due to convergence errors in the flow conditions and the curves were drawn with the method of least squares in the figures. Some points disagree in the figures.

The contraction ratio due to the sidewalls is 1.22, and the duct length upstream of the pseudo-shock is plotted from the ratio of 1.22. As the contraction ratio increases, impulse function and pressure in the downstream combustor section upstream of the downstream throat increase, and the starting position of the pseudo-shock moves upstream. As the rocket chamber pressure increases, the impulse function from the rocket increases and reaction force from the divergent wall should be decreased to meet the outflow impulse function under the choking condition. Then the starting position moves downstream.

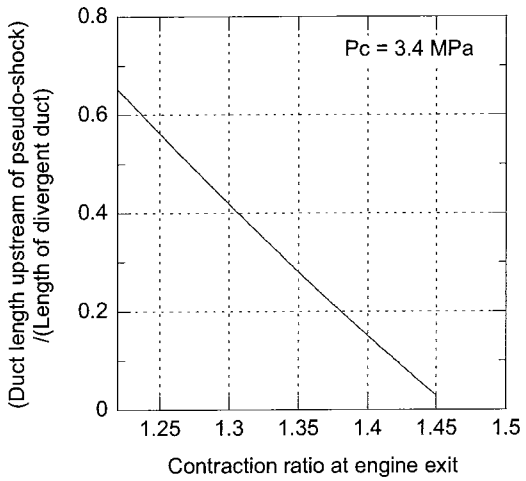

Fig. 18 Effect of the downstream throat contraction ratio on pseudo-shock length.

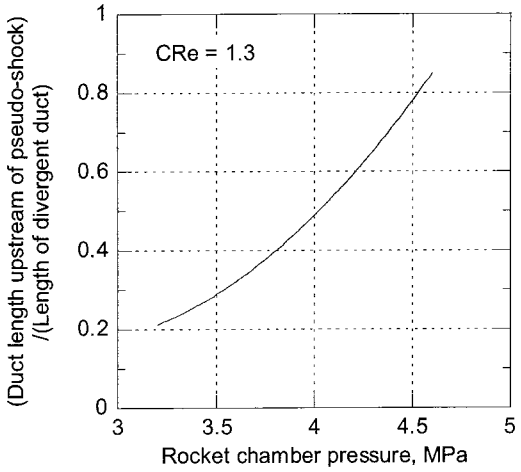

Fig. 19 Effect of rocket chamber pressure on pseudo-shock length.

3.7. Downstream combustor

In the downstream combustion ramjet mode, decelerated subsonic air reacts with fuel injected in the downstream combustor. Rocket exhaust works as pilot flame. This mode was confirmed with combustor tests.[12,27] Figure 20 shows schematic of the experimental model and Figure 21 shows wall pressure and estimated Mach number distributions. The downstream straight duct section was required to attain sufficient combustion efficiency.

In Fig. 4, there is fuel injector only on the top wall of the downstream combustor. In the engine model, there will be several fuel injection positions in the divergent section and on the sidewalls and the cowl.

In the tests, there was no throat at the exit of the model. Even with no throat, combustion gas chokes thermally. This configuration of the divergent section is suitable to the scramjet and the rocket modes. In the new engine model, however, there is a throat at the exit of the model in the ejector-jet and the ramjet modes. Excessive hydrogen fuel is necessary to attain the thermal choking with no throat. This combustion gas with large amount of residual hydrogen fuel is avoided for safety.

Combustor tests were also conducted in the ejector-jet mode.[28] Figure 22 shows the experimental setup. The tests were conducted under the sea-level static air condition. The reference rocket chamber pressure was 3 MPa. Air was breathed into the combustor model by the ejector effect, and wall

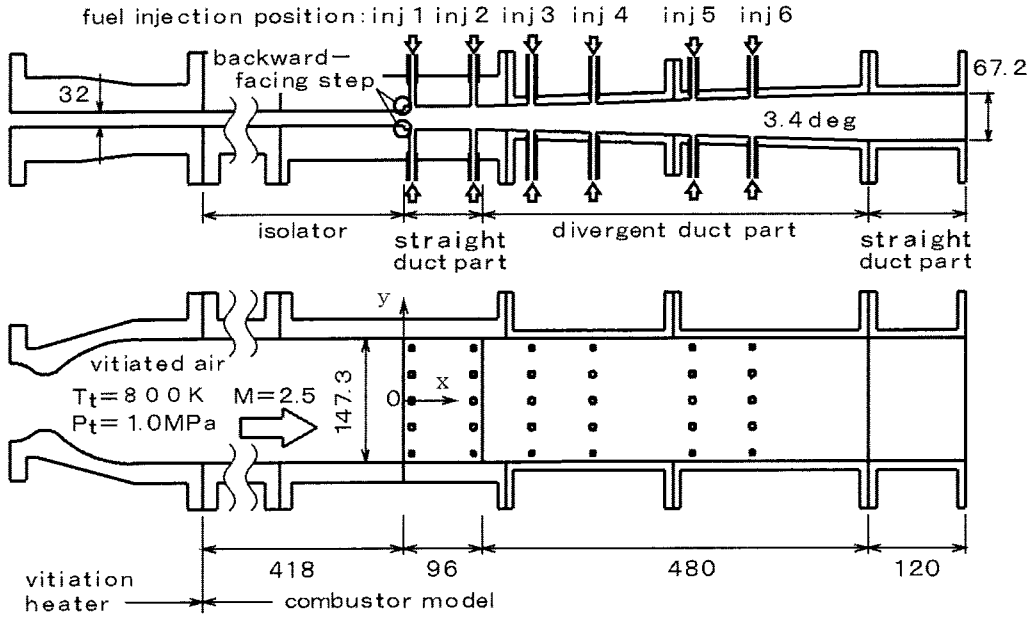

Fig. 20 Schematic of experimental model of downstream-combustion ramjet mode.

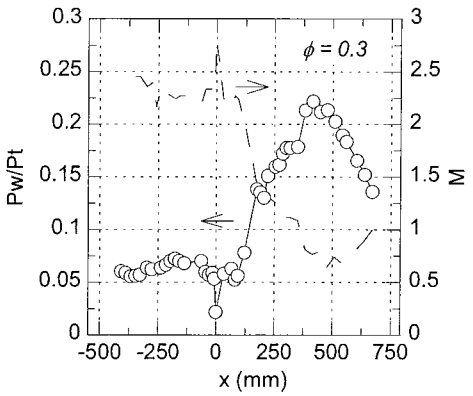

Fig. 21 Wall pressure and estimated Mach number distributions in the downstream combustion ramjet mode.

pressure at the throat section decreased to choking pressure. The rocket exhaust and airflow mixed and the mixture was decelerated in the divergent section. The pressure in the downstream combustor was higher than an atmosphere. Fuel hydrogen was injected to the mixture and the combustion gas choked at the exit throat. Operation of the ejector-jet mode was demonstrated with this model.

3.8. Design of the engine

With the above-mentioned results and works, the duct configuration of the new engine model is designed as shown in Fig. 4. Reference engine configurations are listed in Table 2. The operating conditions are predicted as listed in Table 3. They are calculated with a one-dimensional model with equilibrium condition of gases. EJ is ejector-jet mode, RM is ramjet mode, SC is scramjet mode, and UR is upstream-combustion ramjet mode. In the ejector-jet and ramjet modes, primary combustion of fuel and air progresses in the downstream combustor. In the scramjet and upstream-combustion ramjet modes, it progresses in the upstream combustor. Figure 23 shows maximum pressures and maximum heat fluxes throughout the tests in different Mach number conditions and different operating modes. Number and configuration of the cooling channels and flow rates of cooling water will be specified with the estimated heat fluxes. Thermally equilibrium condition is not designed in cooling, but the engine model is designed to hold for 30 s duration of each test.

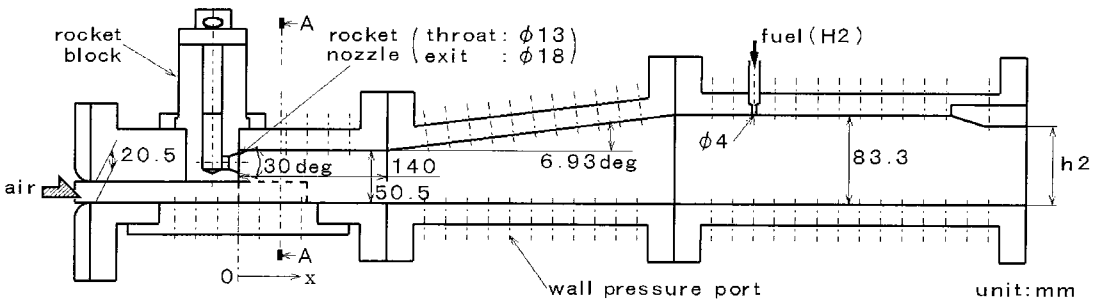

Fig. 22 Schematic of a combustor model of ejector-jet mode.

Table 2 Engine configuration

Length	Width at entrance	Height at entrance	Width in engine	Upstream combustor length	Contraction ratio of inlet	Contraction ratio of upstream combustor	Rocket throat diameter	Rocket nozzle exit diameter
3 m	0.22 m	0.2 m	0.18 m	0.55 m	4.9	1.9	26 mm	70 mm

Table 3 Operating conditions

Airflow condition	Operating mode	Inlet condition	Rocket chamber Pressure, MPa	Rocket O/F	Equivalence ratio for air	Thrust, kN
Static air	EJ	—	3.0	7.0	0.8	3.8
Static air	EJ	—	4.0	7.0	1.0	5.4
M4	EJ	Unstart	3.0	7.0	1.0	0.7
M4	EJ	Srart	3.0	7.0	1.0	6.6
M4	RM	Srart	0.5	5.0	0.4	1.7
M4	UR	Srart	3.0	5.0	1.0	5.8
M6	RM	Srart	0.5	5.0	1.0	1.5
M6	SC	Srart	3.0	5.0	1.1	5.3
M8	SC	Srart	1.5	5.0	1.1	2.5

EJ is ejector-jet mode, RM is ramjet mode, SC is scramjet mode, and UR is upstream-combustion ramjet mode.

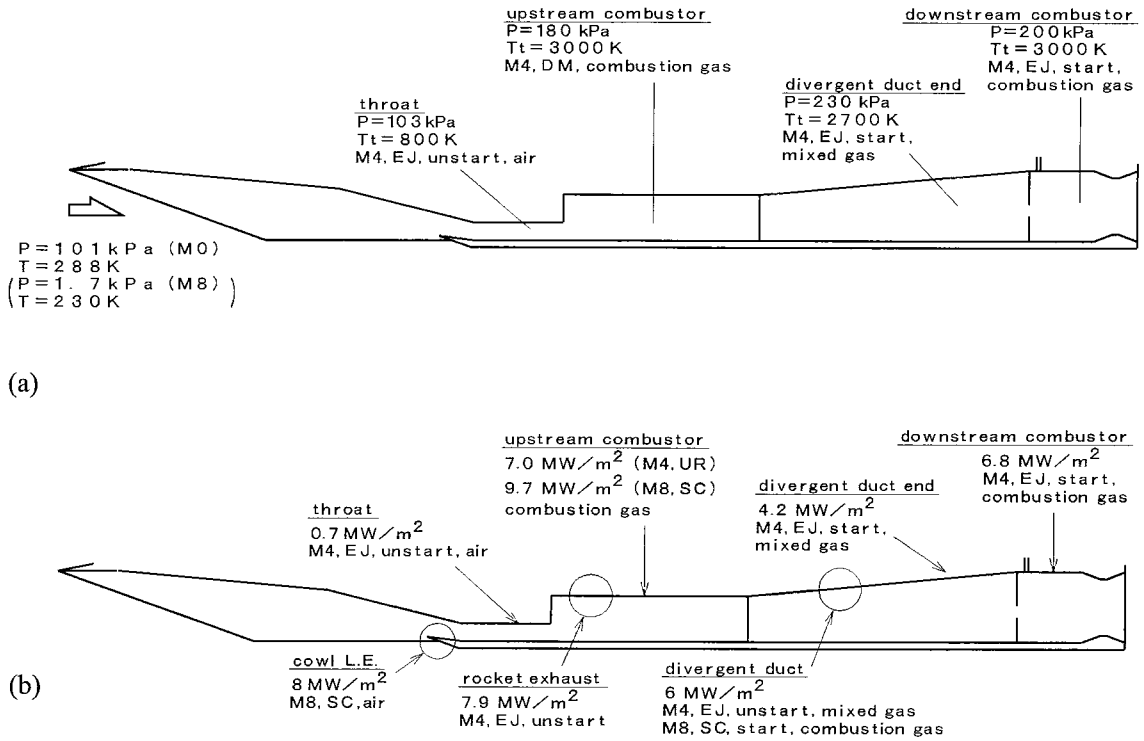

Fig. 23 Maximum pressures and heat fluxes of the engine model throughout operations.
(a) Pressure. (b) Heat flux.

In the tests, rocket chamber pressure and the contraction ratio at the engine exit will be parameters, as well as the fuel injection position. Parts and components of the engine will be manufactured to conduct these parametric studies. The leading edge part of the cowl will be changeable.

4. CLOSING REMARKS

Reference investigation results and design process of the new model of the rocket-ramjet combined cycle engine are presented. The ejector rockets, the upstream throat and upstream combustor section, and the divergent section are now under construction. The inlet section and the downstream combustor section will be constructed in next year. RJTF is also now under modification; adding oxygen feed-line for the rockets, installing a new force measurement system, and adjusting control system. The first objective of the tests is to evaluate its performance in the ejector-jet mode at sea-level static conditions scheduled in FY2006. With the tests at various conditions in RJTF with this engine model, our group will establish design

technologies of the rocket-ramjet combined-cycle engine to realize a future transportation system.

Recent combustion tests and CFD investigation on the ejector effect indicate reduction of the ejector effect from the designed ability due to high temperature of the primary flow. Our succeeding papers and reports on the ejector mode operation should be referred when an engine is designed.

References

1) http://www.jaxa.jp/about/vision_mission/long_term/index_e.html

2) Siebenhaar, A., "Strutjet Evolves to Meet Air-Breathing Propulsion Challenges for the 21st Century," 13th International Symposium on Air-Breathing Engines, Paper 97-7135, Sep. 1997.

3) Andreadis, D., Drake, A., Garrett, J. L., Gettinger, C. D., and Hoxie, S. S., "Design Consideration of ISTAR Hydrocarbon Fueled Combustor Operating Air Augmented Rocket, Ramjet and Scramjet Modes," 11th AIAA/AAAF International Conference on Space Planes and Hypersonic Systems and Technologies Paper, Orleans, France, Sep. 2002.

4) Lee, J., and Krivanek, T., "Design and Fabrication of the ISTAR Direct-Connect Combustor Experiment at the NASA Hypersonic Tunnel Facility," AIAA Paper, AIAA-2005-0611, Jan. 2005.

5) Heiser, W. H., Pratt, D. T., Daley, D. H., and Mehta, U. B., "Hypersonic Airbreathing Propulsion," AIAA Education Series, AIAA, Washington, DC, 1994, pp. 447-451.

6) Kanda, T., and Kudo, K., "Conceptual Study of a Combined-Cycle Engine for an Aerospace Plane," *Journal of Propulsion and Power*, Vol. 19, No. 5, 2003, pp. 859-867.

7) Kanda, T., Chinzei, N., Kudo, K., and Murakami, A., "Dual-Mode Operation in a Scramjet Combustor," *Journal of Propulsion and Power*, Vol. 20, No. 4, 2004, pp. 760-763.

8) Sullins, G. A., "Demonstration of Mode Transition in a Scramjet Combustor," *Journal of Propulsion and Power*, Vo. 9, No. 4, 1993, pp. 515-520.

9) Kanda, T., Kudo, K., Tani, K., and Kato, K., "Calculation of Dual-Mode Engine Performance," *Transactions of JSASS*, Vol. 48, No. 162, 2006, pp. 221-228.

10) Kanda, T., Tani, K., and Kudo, K., "Conceptual Study of a Rocket-Ramjet Combined-Cycle Engine for an Aerospace Plane," *Proceedings of 17th International Symposium on Airbreathing Engines*, International Society for Airbreathing Engines, Munich, Germany, ISABE-2005-1298, Sep. 2005.

11) Kanda, T., and Kudo, K., "Cooling Requirement of Combined Cycle Engine in Descending Flight," *Proceedings of 24th International Symposium on Space Technology and Science*, the Japan Society for Aeronautical and Space Sciences, Miyazaki, Japan, 2004, pp.39-44.

12) Kato, K., Kanda, T., Kobayashi, K., Kudo, K., Murakami, A., "Experimental Study of Downstream Combustion Ramjet-Mode,"AIAA Paper 2005-0617, Jan.2005.

13) Kobayashi, K., Tomioka, S., Kato, K., Murakami, A., Kudo, K., and Mitani, T., "Performance of a Dual-Mode Combustor with Multi-Staged Fuel Injection," AIAA Paper 2004-3482, Jul. 2004.

14) Tani, K., Kanda, T., Kato, K., Sakuranaka, N. and Watanabe, S., "Designing and Aerodynamic Performance of the Combined Cycle Engine in a Hypersonic Flow," 52nd International Aeronautical Congress Paper, IAC-05-C4.5.06, Fukuoka, Japan, Oct. 2005.

15) Kubota, S., Masuya, G., and Tani, K., "Aerodynamic Performances of the Combined Cycle Inlet," 24th International Congress of Aeronautical Sciences Paper ICAS 2004-6.6.1, Yokohama, Japan, Sep. 2004.

16) Ueda, S., Saito, T., and Takegoshi, M., to be presented.

17) Bartz, D. R. "A Simple Equation for Rapid Estimation of Rocket Nozzle Convective Heat Transfer Coefficients," *Jet Propulsion*, 1957, pp.49-51.

18) Ono, F., Tamura, H., Sakamoto, H., and Sasaki, M., "Combustion Characteristics of Oxygen/ Hydrogen High Pressure Preburners for Staged Combustion Cycle Rocket Engine," Technical Report of National Aerospace Laboratory TR-1044, Nov. 1989. (in Japanese)

19) Calhoon, D. F.,. Ito, J. I., and Kors, K. L., 'Handbook for Design of Gaseous Propellant Injectors and Combustion Chambers,' NASA Lewis Research Center Contract, NAS 3-14379, 1973.

20) Niino, M., Kumakawa, A., Yatsuyanagi, N., Gomi, H., Suzuki, A., Sakamoto, H., Sasaki, M., and Yanagawa, K., "A Study on Heat Transfer Characteristics of Water Cooled LO2/LH2 Rocket Combustor," Technical Report of National Aerospace Laboratory TR-708, May 1982. (in Japanese)
21) Takegoshi, M., Tomioka, S., Ueda, S., Saito, T., Izumikawa, M., and Hayasaka, O., "Firing –Tests of a Rocket Combustor for Combined Cycle Engine at Various Conditions," AIAA Paper 2005-4286, Jul. 2005.
22) Aoki, S., Lee, J., Msuya, G., Kanda, T., and Kudo, K., "Aerodynamic Experiment of an Ejector-Jet," *Journal of Propulsion and Power*, Vol. 21, No. 3, 2005, pp. 496-503.
23) Tani, K., Kanda, T., and Tokudome, S., "Aerodynamic Characteristics of the Combined Cycle Engine in an Ejector Jet Mode," AIAA 2005-1210, Jan. 2005.
24) Kato, K., Kanda, T., Kudo, K., and Murakami, A., "Experimental Study of Combined Cycle Engine Combustor in Scramjet-Mode," AIAA Paper 2005-3316, May 2005.
25) Tomioka, S., Kudo, K., Murakami, A., and Kanda, T., "Auxiliary Injection for Combustion Augmentation of G/G Plume in a RBCC Combustor," AIAA Paper 2005-4284, Jul. 2005.
26) Kanda, T., and Tani, K., "Momentum Balance Model of Flow Field with Pseudo-Shock," AIAA Paper 2005-1045, Jan. 2005.
27) Kato, K., Kanda, T., Kobayashi, K., Kudo, K., and Murakami, A., "Ramjet-mode Operation in a Combined-Cycle Engine Combustor," Joint Conference on Space Sciences and Technologies Paper, Japan Society for Aeronautical and Space Sciences, 2G11, Nov. 2005. (in Japanese)
28) Kanda, T., Tani, K., Kato, K., Kudo, K., and Murakami, A., "Experimental Study of a Combined-Cycle Engine Combustor in Ejector-Jet Mode," AIAA Paper 2006-0223, Jan. 2006.

JAXA Research and Development Report JAXA-RR-06-009E

Date of Issue : February 28, 2007
Edited and Published by : Japan Aerospace Exploration Agency
7-44-1 Jindaiji-higashimachi, Chofu-shi, Tokyo 182-8522 Japan
URL: http://www.jaxa.jp/
Printed by : BCC Co., Ltd.